PERGAMON

International Journal of Heat and Mass Transfer 45 (2002) 3529–3547

International Journal of HEAT and MASS TRANSFER

www.elsevier.com/locate/ijhmt

# Improvement in performance of multi-pass laminar counterflow heat exchangers with external refluxes

Chii-Dong Ho *, Ho-Ming Yeh, Yu-Chuan Tsai

*Department of Chemical Engineering, Tamkang University, Tamsui, Taipei 251, Taiwan, ROC*

Received 17 April 2001; received in revised form 7 February 2002

**Abstract**

A study on improvement in performance of multi-pass rectangular heat exchangers with uniform wall temperature and with external refluxes has been carried out under counterflow operations. An orthogonal expansion technique for solving such a conjugated Graetz problem is developed and applied to investigate a substantially improving heat transfer. A description of the average Nusselt number and the outlet dimensionless temperature is given. It is shown that for asymptotic average Nusselt numbers exit in counterflow as in single-flow operations. Numerical values of asymptotic average Nusselt numbers are reported for a wide range of Graetz numbers. Comparisons of analytical results are made with single-flow operations of the same size (without sheets inserted and without recycle). Considerable improvement in the heat transfer rate for large Graetz numbers is obtainable by introducing the recycle-effect concept in designing such double-pass operations. The effect of sheet location on the enhancement of heat transfer efficiency as well as on the increment of power consumption has been also discussed. 

## 1. Introduction

Dealing with laminar forced convection heat transfer in a bounded duct ignoring axial conduction is known as the Graetz problem [1,2], while such problems are extended to low Prandtl number fluids such as liquid metals, referred to the extended Graetz problem [3–6], the assumption of negligible axial conduction is not always valid. The extension of single-stream problems to multistream or multiphase systems with coupling through mutual conditions at the boundaries is expected, as in conjugated Graetz problems. Perelman [7] used a general theory of equations to solve hyperbolic–elliptic conjugated problems. Murkerjee and Davis [8] derived a simple method to analyze the temperature distribution of a stratified two-phase laminar flow. The conjugated boundary-value problem involving chemical reaction in hollow-fiber enzyme reactor was studied by Kim and Coony [9], while another conjugated boundary-value problems in chemical engineering application were treated by Davis and Venkatesh [10]. Among problems involving any dual combination of fluid and solid phases, Papoutsakis and Ramkrishna [11,12] have developed and presented a general formalism. Yin and Bau [13] used eigenfunction expansion techniques to solve the simultaneous energy equations in the fluid and the solid regions.

A new device, with increasing the fluid velocity but the heat-transfer area as well as the aspect ratio kept unchanged, was introduced by inserting the parallel impermeable sheets in the flow channel to divide it into four subchannels. The analytical solution for solving such devices with external refluxes is obtainable by the use of an orthogonal expansion technique [14–16]. The mathematical formulation derived by means of this technique was employed broadly and successfully by many investigators [17–24], and came out with an infinite number of eigenvalues and only the first negative eigenvalue was considered for the rapid convergence in the present paper. Applications of the recycle-effect

* Corresponding author. Tel.: +886-2-26266632; fax: +886-2-26209887.
*E-mail address:* cdho@mail.tku.edu.tw (C.-D. Ho).

0017-9310/02/$ - see front matter 
PII: S0017-9310(02)00070-4

**Nomenclature**

| | |
|---|---|
| $B$ | conduit width, m |
| $c_p$ | specific heat at constant pressure, kJ/kg K |
| $D_e$ | equivalent diameter of conduit, m |
| $F_m$ | eigenfunction associated with eigenvalue $\lambda_m$ |
| $f$ | friction factor |
| $Gz$ | Graetz number, $VW/\alpha BL$ |
| $G_m$ | function defined during the use of orthogonal expansion method |
| $\bar{h}$ | average heat transfer coefficient, kW/m$^2$ K |
| $I_h$ | improvement of heat transfer, defined by Eq. (51) |
| $I_p$ | increment of power consumption, defined by Eq. (58) |
| $k$ | thermal conductivity of the fluid, kW/m K |
| L | conduit length, m |
| $\ell w_f$ | friction loss in conduit, m$^2$/s$^2$ |
| $\overline{Nu}$ | Nusselt number |
| $p_{mn}$ | coefficient in the eigenfunction $F_{a,m}$ |
| $q$ | heat transfer rate, kW |
| $q_{mn}$ | coefficient in the eigenfunction $F_{b,m}$ |
| $r_{mn}$ | coefficient in the eigenfunction $F_{c,m}$ |
| $R$ | reflux ratio, reverse volume flow rate divided by input volume flow rate |
| $Re$ | Reynolds number |
| $S_m$ | expansion coefficient associated with eigenvalue $\lambda_m$ |
| $t_{mn}$ | coefficient in the eigenfunction $F_{d,m}$ |
| $T$ | temperature of fluid, K |
| $V$ | input volume flow rate of conduit, m$^3$/s |
| $v$ | velocity distribution of fluid, m/s |
| $\overline{v}$ | average velocity of fluid, m/s |
| W | distance between two parallel plates, m |
| $x$ | transversal coordinate, m |
| $z$ | longitudinal coordinate, m |

*Greek symbols*

| | |
|---|---|
| $\alpha$ | thermal diffusivity of fluid, m$^2$/s |
| $\beta$ | ratio of channel thickness, $W_a/W_b = W_d/W_c$ |
| $\Delta$ | ratio of channel thickness, $W_a/W$ |
| $\eta$ | transversal coordinate, $x/W$ |
| $\theta$ | dimensionless temperature, $(T - T_I)/(T_s - T_I)$ |
| $\lambda_m$ | eigenvalue |
| $\xi$ | longitudinal coordinate, $z/L$ |
| $\rho$ | density of the fluid, kg/m$^3$ |
| $\psi$ | dimensionless temperature, $(T - T_s)/(T_I - T_s)$ |

*Subscripts*

| | |
|---|---|
| a | in the channel a |
| b | in the channel b |
| c | in the channel c |
| d | in the channel d |
| F | at the outlet, $\xi = 0$ |
| I | at the inlet |
| L | at the outlet, $\xi = 1$ |
| 0 | in a single-pass device without recycle |
| s | at the wall surface |

concept to separation processes and reactor designs with external or internal refluxes have led to improved performance, and widely used in absorption, fermentation, and polymerization, such as loop reactors [25,26], air-lift reactors [27,28] and draft-tube bubble columns [29,30].

The purposes of the present study are an extension of the previous works [15,16] to investigate the improvement of performance and to develop an orthogonal expansion technique to the heat transfer in multi-pass heat exchangers by inserting several impermeable sheets with negligible thermal resistance with external refluxes. The solutions to such problems are obtained by the use of the method of separation of variables, where the resulting eigenvalue problem is solved by the orthogonality conditions. The effect of impermeable-sheet position on the improvement of transfer efficiency with reflux ratio and Graetz number as parameters as well as on the increment of power consumption was also discussed.

## 2. Temperature distributions in a multi-pass device with recycle

Three impermeable sheets with negligible thermal resistance are inserted in parallel into a parallel-plate channel with thickness $W$, length $L$, and width $B$ ($\gg W$) to divide the open duct into four parts, channels a, b, c and d with thickness $W_a$, $W_b$, $W_c$ and $W_d$, respectively, and the ratio of channel thickness is defined as $\beta = W_a/W_b = W_d/W_c$. Before entering each of the two inner tubes for a four-pass operation (flow pattern A) as shown in Fig. 1(a), the fluid with volume flow rate $V$ and the inlet temperature $T_I$ will mix with the fluid exiting from the inner tube with the volume flow rate $RV$ and the outlet temperature $T_F$, which is regulated by using a conventional pump. The inlet fluid may flow through two outer tubes with mixing the external reflux exiting from the outer tube (flow pattern B) as shown in Fig. 1(b). In each flow pattern, the fluid is completely mixed at the inlet and outlet of the tube.

After the following assumptions are made: constant physical properties and wall temperature, purely fully developed laminar flow in each channel, and negligible axial diffusion as well as entrance length and end effects, the velocity distributions and equations of energy in dimensionless from may be obtained as

$$\frac{\partial^2\psi_i(\eta_i,\xi)}{\partial\eta_i^2} = \left[\frac{W_i^2 v(\eta_i)}{L\alpha}\right]\frac{\partial\psi_i(\eta_i,\xi)}{\partial\xi}, \quad i = \mathrm{a,b,c,d}, \tag{1}$$

$$v_i(\eta_i) = \overline{v_i}(6\eta_i - 6\eta_i^2), \quad 0 \leqslant \eta_i \leqslant 1, \quad i = \mathrm{a,b,c,d} \tag{2}$$

in which

$$\overline{v_\mathrm{a}} = -[V/W_\mathrm{a}B], \quad \overline{v_\mathrm{b}} = [(R+1)V/W_\mathrm{b}B], \quad \overline{v_\mathrm{c}} = [(R+1)V/W_\mathrm{c}B], \quad \overline{v_\mathrm{d}} = -[V/W_\mathrm{d}B], \quad \eta_i = \frac{x_i}{W_i}, \quad \xi = \frac{z}{L},$$
$$\psi_i = \frac{T_i - T_\mathrm{s}}{T_\mathrm{I} - T_\mathrm{s}}, \quad \theta_i = 1 - \psi_i = \frac{T_i - T_\mathrm{I}}{T_\mathrm{s} - T_\mathrm{I}}, \quad W_\mathrm{a} = W_\mathrm{d}, \quad W_\mathrm{b} = W_\mathrm{c}, \quad Gz = \frac{V(W_\mathrm{a}+W_\mathrm{b}+W_\mathrm{c}+W_\mathrm{d})}{\alpha BL} = \frac{VW}{\alpha BL},$$
$$i = \mathrm{a,b,c,d}. \tag{3}$$

The boundary conditions for solving Eqs. (1) and (2) are

$$\psi_\mathrm{a}(0,\xi) = 0, \tag{4}$$

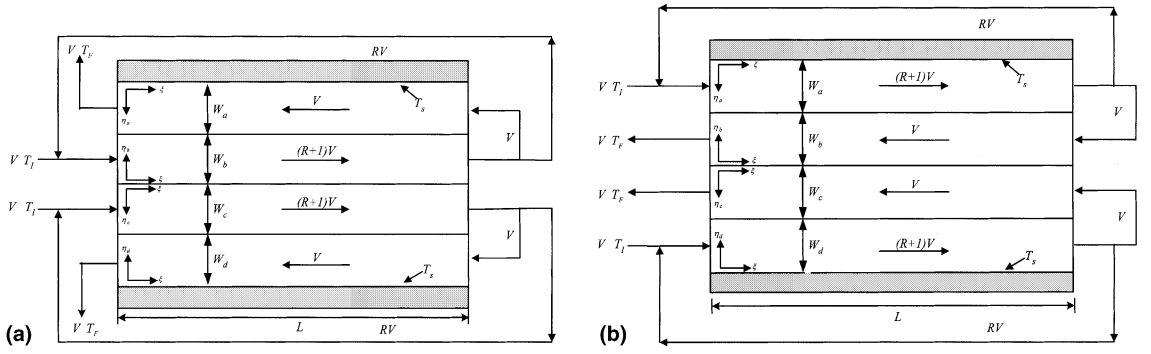


Fig. 1. Multi-pass parallel-plate heat exchangers with external refluxes at both ends: (a) flow pattern A; (b) flow pattern B.

$$\psi_a(1,\xi) = \psi_b(1,\xi), \tag{5}$$

$$-\frac{\partial\psi_a(1,\xi)}{\partial\eta_a} = \frac{W_a}{W_b}\frac{\partial\psi_b(1,\xi)}{\partial\eta_b}, \tag{6}$$

$$\psi_b(0,\xi) = \psi_c(0,\xi), \tag{7}$$

$$-\frac{\partial\psi_b(0,\xi)}{\partial\eta_b} = \frac{W_b}{W_c}\frac{\partial\psi_c(0,\xi)}{\partial\eta_c}, \tag{8}$$

$$\psi_c(1,\xi) = \psi_d(1,\xi), \tag{9}$$

$$-\frac{\partial\psi_c(1,\xi)}{\partial\eta_c} = \frac{W_c}{W_d}\frac{\partial\psi_d(1,\xi)}{\partial\eta_d}, \tag{10}$$

$$\psi_d(0,\xi) = 0 \tag{11}$$

and the dimensionless outlet temperature is

$$\theta_F = 1 - \psi_F = \frac{T_F - T_I}{T_s - T_I}. \tag{12a}$$

Inspection of Eqs. (1), (2) and (4)–(11) shows that the inlet conditions for four channels are not specified a priori and reverse flow occurs. The analytical solutions to both flow patterns may be obtained by the use of an orthogonal expansion technique with the eigenfunction expanding in terms of an extended power series.

Separation of variables in the form

$$\psi_i(\eta_i,\xi) = \sum_{m=0}^{\infty} S_{i,m}F_{i,m}(\eta_i)G_m(\xi), \quad i = a,b,c,d \tag{12b}$$

applied to Eqs. (1) and (2) leads to

$$G_m(\xi) = e^{-\lambda_m(1-\xi)}, \tag{13}$$

$$F''_{i,m}(\eta_i) - \left[\frac{\lambda_m W_i^2 v_i(\eta_i)}{L\alpha}\right]F_{i,m}(\eta_i) = 0, \quad i = a,b,c,d \tag{14}$$

and also the boundary conditions in Eqs. (4)–(11) can be rewritten as

$$F_{a,m}(0) = 0, \tag{15}$$

$$S_{a,m}F_{a,m}(1) = S_{b,m}F_{b,m}(1), \tag{16}$$

$$S_{a,m}F'_{a,m}(1) = -\frac{W_a}{W_b}S_{b,m}F'_{b,m}(1), \tag{17}$$

$$S_{b,m}F_{b,m}(0) = S_{c,m}F_{c,m}(0), \tag{18}$$

$$S_{b,m}F'_{b,m}(0) = -\frac{W_b}{W_c}S_{c,m}F'_{c,m}(0), \tag{19}$$

$$S_{c,m}F_{c,m}(1) = S_{d,m}F_{d,m}(1), \tag{20}$$

$$S_{c,m}F'_{c,m}(1) = -\frac{W_c}{W_d}S_{d,m}F'_{d,m}(1), \tag{21}$$

$$F_{d,m}(0) = 0, \tag{22}$$

where the primes on $F_{a,m}(\eta_a)$, $F_{b,m}(\eta_b)$, $F_{c,m}(\eta_c)$ and $F_{d,m}(\eta_d)$ denote the differentiations with respect to $\eta_a$, $\eta_b$, $\eta_c$ and $\eta_d$, respectively.

Combinations of Eqs. (16) and (17), Eqs. (18) and (19), and Eqs. (20) and (21) result in Eqs. (27)–(29), respectively

$$\frac{F_{a,m}(1)}{F'_{a,m}(1)} = -\frac{W_b F_{b,m}(1)}{W_a F'_{b,m}(1)}, \tag{27}$$

$$\frac{F_{b,m}(0)}{F'_{b,m}(0)} = -\frac{W_c F_{c,m}(0)}{W_b F'_{c,m}(0)}, \tag{28}$$

$$\frac{F_{c,m}(1)}{F'_{c,m}(1)} = -\frac{W_d F_{d,m}(1)}{W_c F'_{d,m}(1)} \tag{29}$$

in which the eigenfunctions $F_{a,m}(\eta_a)$, $F_{b,m}(\eta_b)$, $F_{c,m}(\eta_c)$ and $F_{d,m}(\eta_d)$ were assumed to be polynomials to avoid the loss of generality. With the use of Eqs. (15) and (22), we have

$$F_{a,m}(\eta_a) = \sum_{n=0}^{\infty} p_{m,n}\eta_a^n, \quad p_{m,0} = 0,\ p_{m,1} = 1 \quad \text{(selected)}, \tag{23}$$

$$F_{b,m}(\eta_b) = \sum_{n=0}^{\infty} q_{m,n}\eta_b^n, \quad q_{m,0} = 1 \quad \text{(selected)}, \tag{24}$$

$$F_{c,m}(\eta_c) = \sum_{n=0}^{\infty} r_{m,n}\eta_c^n, \quad r_{m,0} = 1 \quad \text{(selected)}, \tag{25}$$

$$F_{d,m}(\eta_d) = \sum_{n=0}^{\infty} t_{m,n}\eta_d^n, \quad t_{m,0} = 0,\ t_{m,1} = 1 \quad \text{(selected)}. \tag{26}$$

Substituting Eqs. (23)–(26) into (14), all the coefficients $p_{m,n}$, $q_{m,n}$, $r_{m,n}$ and $t_{m,n}$ may be expressed in terms of eigenvalues $\lambda_m$ after using Eqs. (15) and (22), as referred to in Appendix A. Therefore, it is easy to solve all eigenvalues from Eqs. (27)–(29) and the eigenfunctions associated with the corresponding eigenvalues are also well defined by Eqs. (23)–(26). These eigenvalues, $\lambda_m$, thus calculated, include a positive set, a negative set and a complex set, each of which is required for the counterflow system, the eigenvalues indicated in Table 1 are the set dominant in the system.

A demonstration of completeness and its justification based on Sturm–Liouville theorem have been developed, as referred to in Appendix B, and the orthogonality conditions can be expressed as follows:

$$\begin{aligned} &W_b W_c W_d \int_0^1 \left[\frac{W_a^2 v_a(\eta_a)}{L\alpha}\right] S_{a,m}S_{a,n}F_{a,n}F_{a,m}\,d\eta_a + W_c W_d W_a \int_0^1 \left[\frac{W_b^2 v_b(\eta_b)}{L\alpha}\right] S_{b,m}S_{b,n}F_{b,n}F_{b,m}\,d\eta_b + W_d W_a W_b \\ &\times \int_0^1 \left[\frac{W_c^2 v_c(\eta_c)}{L\alpha}\right] S_{c,m}S_{c,n}F_{c,n}F_{c,m}\,d\eta_c + W_a W_b W_c \int_0^1 \left[\frac{W_d^2 v_d(\eta_d)}{L\alpha}\right] S_{d,m}S_{d,n}F_{d,n}F_{d,m}\,d\eta_d \\ &= 0 \end{aligned} \tag{30}$$

when $n \neq m$. Since

$$\psi_{L,ab} = \sum_{m=0}^{\infty} S_{a,m}F_{a,m}(\eta_a) = \sum_{m=0}^{\infty} S_{b,m}F_{b,m}(\eta_b), \tag{31}$$

$$\psi_{L,cd} = \sum_{m=0}^{\infty} S_{c,m}F_{c,m}(\eta_c) = \sum_{m=0}^{\infty} S_{d,m}F_{d,m}(\eta_d). \tag{32}$$

Table 1
Eigenvalues and expansion coefficients as well as dimensionless outlet temperatures in double-pass devices with recycle for $\beta = 1$ and $R = 1$; $Gz\,\lambda_0 = -1.5605$ and $Gz\,\lambda_1 = -89.9486$ (flow pattern A)

| $Gz$ | $m$ | $\lambda_m$ | $S_{a,m}$ | $S_{b,m}$ | $S_{c,m}$ | $S_{d,m}$ | $\psi_F(\lambda_0)$ | $\psi_F(\lambda_0,\lambda_1)$ |
|---|---|---|---|---|---|---|---|---|
| 1 | 0 | −1.5605 | $8.3\times10^{-2}$ | $4.7\times10^{-2}$ | $4.7\times10^{-2}$ | $8.3\times10^{-2}$ | 0.2029 | 0.2029 |
| | 1 | −89.9486 | $3.5\times10^{-46}$ | $7.1\times10^{-12}$ | $7.1\times10^{-12}$ | $-2.9\times10^{-46}$ | | |
| 10 | 0 | −0.1560 | $9.7\times10^{-1}$ | $5.5\times10^{-1}$ | $5.5\times10^{-1}$ | $9.7\times10^{-1}$ | 0.5819 | 0.5819 |
| | 1 | −8.9949 | $-4.8\times10^{-12}$ | $-3.7\times10^{-11}$ | $-3.7\times10^{-11}$ | $-4.8\times10^{-12}$ | | |
| 100 | 0 | −0.0156 | 1.7733 | 1.0125 | 1.0125 | 1.7733 | 0.9285 | 0.9285 |
| | 1 | −0.8995 | $-1.5\times10^{-7}$ | $-8.2\times10^{-10}$ | $-8.2\times10^{-10}$ | $-1.5\times10^{-7}$ | | |
| 1000 | 0 | −0.0016 | 1.9219 | 1.0974 | 1.0974 | 1.9219 | 0.9923 | 0.9923 |
| | 1 | −0.0899 | $1.3\times10^{-7}$ | $1.2\times10^{-9}$ | $1.2\times10^{-9}$ | $1.3\times10^{-7}$ | | |

From the orthogonality conditions, the general expressions for the expansion coefficients may be obtained. Accordingly, we have

$$\begin{aligned}
&W_{\mathrm{b}}W_{\mathrm{c}}W_{\mathrm{d}}\int_0^1 \psi_{\mathrm{L,ab}}\left[\frac{W_{\mathrm{a}}^2 v_{\mathrm{a}}(\eta_{\mathrm{a}})}{L\alpha}\right]S_{\mathrm{a},m}F_{\mathrm{a},m}\,\mathrm{d}\eta_{\mathrm{a}} + W_{\mathrm{c}}W_{\mathrm{d}}W_{\mathrm{a}}\int_0^1 \psi_{\mathrm{L,ab}}\left[\frac{W_{\mathrm{b}}^2 v_{\mathrm{b}}(\eta_{\mathrm{b}})}{L\alpha}\right]S_{\mathrm{b},m}F_{\mathrm{b},m}\,\mathrm{d}\eta_{\mathrm{b}}\\
&\quad + W_{\mathrm{d}}W_{\mathrm{a}}W_{\mathrm{b}}\int_0^1 \psi_{\mathrm{L,cd}}\left[\frac{W_{\mathrm{c}}^2 v_{\mathrm{c}}(\eta_{\mathrm{c}})}{L\alpha}\right]S_{\mathrm{c},m}F_{\mathrm{c},m}\,\mathrm{d}\eta_{\mathrm{c}} + W_{\mathrm{a}}W_{\mathrm{b}}W_{\mathrm{c}}\int_0^1 \psi_{\mathrm{L,cd}}\left[\frac{W_{\mathrm{d}}^2 v_{\mathrm{d}}(\eta_{\mathrm{d}})}{L\alpha}\right]S_{\mathrm{d},m}F_{\mathrm{d},m}\,\mathrm{d}\eta_{\mathrm{d}}\\
&= W_{\mathrm{b}}W_{\mathrm{c}}W_{\mathrm{d}}\int_0^1 S_{\mathrm{a},m}^2\left[\frac{W_{\mathrm{a}}^2 v_{\mathrm{a}}(\eta_{\mathrm{a}})}{L\alpha}\right]F_{\mathrm{a},m}^2\,\mathrm{d}\eta_{\mathrm{a}} + W_{\mathrm{c}}W_{\mathrm{d}}W_{\mathrm{a}}\int_0^1 S_{\mathrm{b},m}^2\left[\frac{W_{\mathrm{b}}^2 v_{\mathrm{b}}(\eta_{\mathrm{b}})}{L\alpha}\right]F_{\mathrm{b},m}^2\,\mathrm{d}\eta_{\mathrm{b}}\\
&\quad + W_{\mathrm{d}}W_{\mathrm{a}}W_{\mathrm{b}}\int_0^1 S_{\mathrm{c},m}^2\left[\frac{W_{\mathrm{c}}^2 v_{\mathrm{c}}(\eta_{\mathrm{c}})}{L\alpha}\right]F_{\mathrm{c},m}^2\,\mathrm{d}\eta_{\mathrm{c}} + W_{\mathrm{a}}W_{\mathrm{b}}W_{\mathrm{c}}\int_0^1 S_{\mathrm{d},m}^2\left[\frac{W_{\mathrm{d}}^2 v_{\mathrm{d}}(\eta_{\mathrm{d}})}{L\alpha}\right]F_{\mathrm{d},m}^2\,\mathrm{d}\eta_{\mathrm{d}}.
\end{aligned}\tag{33}$$

Eq. (33) can be rewritten as

$$\begin{aligned}
&\psi_{\mathrm{L,ab}}\left[\frac{W_{\mathrm{b}}W_{\mathrm{c}}W_{\mathrm{d}}S_{\mathrm{a},m}}{\lambda_m}\left\{F'_{\mathrm{a},m}(1)-F'_{\mathrm{a},m}(0)\right\} + \frac{W_{\mathrm{c}}W_{\mathrm{d}}W_{\mathrm{a}}S_{\mathrm{b},m}}{\lambda_m}\left\{F'_{\mathrm{b},m}(1)-F'_{\mathrm{b},m}(0)\right\}\right]\\
&\quad + \psi_{\mathrm{L,cd}}\left[\frac{W_{\mathrm{d}}W_{\mathrm{a}}W_{\mathrm{b}}S_{\mathrm{c},m}}{\lambda_m}\left\{F'_{\mathrm{c},m}(1)-F'_{\mathrm{c},m}(0)\right\} + \frac{W_{\mathrm{a}}W_{\mathrm{b}}W_{\mathrm{c}}S_{\mathrm{d},m}}{\lambda_m}\left\{F'_{\mathrm{d},m}(1)-F'_{\mathrm{d},m}(0)\right\}\right]\\
&= W_{\mathrm{b}}W_{\mathrm{c}}W_{\mathrm{d}}S_{\mathrm{a},m}^2\left[F_{\mathrm{a},m}(1)\frac{\partial F'_{\mathrm{a},m}(1)}{\partial\lambda_m} - F'_{\mathrm{a},m}(1)\frac{\partial F_{\mathrm{a},m}(1)}{\partial\lambda_m} + F'_{\mathrm{a},m}(0)\frac{\partial F_{\mathrm{a},m}(0)}{\partial\lambda_m}\right]\\
&\quad + W_{\mathrm{c}}W_{\mathrm{d}}W_{\mathrm{a}}S_{\mathrm{b},m}^2\left[F_{\mathrm{b},m}(1)\frac{\partial F'_{\mathrm{b},m}(1)}{\partial\lambda_m} - F'_{\mathrm{b},m}(1)\frac{\partial F_{\mathrm{b},m}(1)}{\partial\lambda_m} + F'_{\mathrm{b},m}(0)\frac{\partial F_{\mathrm{b},m}(0)}{\partial\lambda_m}\right]\\
&\quad + W_{\mathrm{a}}W_{\mathrm{d}}W_{\mathrm{b}}S_{\mathrm{c},m}^2\left[F_{\mathrm{c},m}(1)\frac{\partial F'_{\mathrm{c},m}(1)}{\partial\lambda_m} - F'_{\mathrm{c},m}(1)\frac{\partial F_{\mathrm{c},m}(1)}{\partial\lambda_m} + F'_{\mathrm{c},m}(0)\frac{\partial F_{\mathrm{c},m}(0)}{\partial\lambda_m}\right]\\
&\quad + W_{\mathrm{a}}W_{\mathrm{b}}W_{\mathrm{c}}S_{\mathrm{d},m}^2\left[F_{\mathrm{d},m}(1)\frac{\partial F'_{\mathrm{d},m}(1)}{\partial\lambda_m} - F'_{\mathrm{d},m}(1)\frac{\partial F_{\mathrm{d},m}(1)}{\partial\lambda_m} + F'_{\mathrm{d},m}(0)\frac{\partial F_{\mathrm{d},m}(0)}{\partial\lambda_m}\right].
\end{aligned}\tag{34}$$

Also, the temperatures at $\xi = 1$ for flow pattern A may also be calculated as follows:

$$\begin{aligned}
\psi_{\mathrm{L,ab}} &= \frac{\int_0^1 v_{\mathrm{b}}W_{\mathrm{b}}B\psi_{\mathrm{b}}(\eta_{\mathrm{b}},1)\,\mathrm{d}\eta_{\mathrm{b}}}{V} = \frac{W}{W_{\mathrm{b}}Gz}\sum_{m=0}^{\infty}\frac{S_{\mathrm{b},m}}{\lambda_m}\left\{F'_{\mathrm{b},m}(1)-F'_{\mathrm{b},m}(0)\right\} = \frac{-\int_0^1 v_{\mathrm{a}}W_{\mathrm{a}}B\psi_{\mathrm{a}}(\eta_{\mathrm{a}},1)\,\mathrm{d}\eta_{\mathrm{a}}}{V(R+1)}\\
&= \frac{-W}{W_{\mathrm{a}}(R+1)Gz}\sum_{m=0}^{\infty}\frac{S_{\mathrm{a},m}}{\lambda_m}\left\{F'_{\mathrm{a},m}(1)-F'_{\mathrm{a},m}(0)\right\}
\end{aligned}\tag{35}$$

and

$$\begin{aligned}
\psi_{\mathrm{L,cd}} &= \frac{\int_0^1 v_{\mathrm{c}}W_{\mathrm{c}}B\psi_{\mathrm{c}}(\eta_{\mathrm{c}},1)\,\mathrm{d}\eta_{\mathrm{c}}}{V} = \frac{W}{W_{\mathrm{c}}Gz}\sum_{m=0}^{\infty}\frac{S_{\mathrm{c},m}}{\lambda_m}\left\{F'_{\mathrm{c},m}(1)-F'_{\mathrm{c},m}(0)\right\} = \frac{-\int_0^1 v_{\mathrm{d}}W_{\mathrm{d}}B\psi_{\mathrm{d}}(\eta_{\mathrm{d}},1)\,\mathrm{d}\eta_{\mathrm{d}}}{V(R+1)}\\
&= \frac{-W}{W_{\mathrm{d}}(R+1)Gz}\sum_{m=0}^{\infty}\frac{S_{\mathrm{d},m}}{\lambda_m}\left\{F'_{\mathrm{d},m}(1)-F'_{\mathrm{d},m}(0)\right\}.
\end{aligned}\tag{36}$$

In Eq. (35) the terms, $\int_0^1 v_{\mathrm{b}}W_{\mathrm{b}}B\psi_{\mathrm{b}}(\eta_{\mathrm{b}},1)\,\mathrm{d}\eta_{\mathrm{b}}$ and $-\int_0^1 v_{\mathrm{a}}W_{\mathrm{a}}B\psi_{\mathrm{a}}(\eta_{\mathrm{a}},1)\,\mathrm{d}\eta_{\mathrm{a}}$, denote the inlet stream of channel b and the outlet stream of channel a, respectively; in Eq. (36) the terms, $\int_0^1 v_{\mathrm{c}}W_{\mathrm{c}}B\psi_{\mathrm{c}}(\eta_{\mathrm{c}},1)\,\mathrm{d}\eta_{\mathrm{c}}$ and $-\int_0^1 v_{\mathrm{d}}W_{\mathrm{d}}B\psi_{\mathrm{d}}(\eta_{\mathrm{d}},1)\,\mathrm{d}\eta_{\mathrm{d}}$, denote the inlet stream of channel c and the outlet stream of channel d, respectively. Accordingly, once all the eigenvalues are found the possible associated expansion coefficients, $S_{\mathrm{a},m}$, $S_{\mathrm{b},m}$, $S_{\mathrm{c},m}$ and $S_{\mathrm{d},m}$ can be calculated from Eqs. (16), (18), (20) and (34)–(36) with $\psi_{\mathrm{L,ab}}$ and $\psi_{\mathrm{L,cd}}$ as intermediate variables during the calculation procedure. Therefore, the dimensionless outlet temperature $\psi_{\mathrm{F,ab}}$ or $\psi_{\mathrm{F,cd}}$ which is referred to as the bulk temperature for flow pattern A, may be calculated by

$$\psi_{\mathrm{F,ab}} = \frac{-\int_0^1 v_{\mathrm{a}}W_{\mathrm{a}}B\psi_{\mathrm{a}}(\eta_{\mathrm{a}},0)\,\mathrm{d}\eta_{\mathrm{a}}}{V} = \frac{-W}{W_{\mathrm{a}}Gz}\sum_{m=0}^{\infty}\frac{\mathrm{e}^{-\lambda_m}S_{\mathrm{a},m}}{\lambda_m}\left\{F'_{\mathrm{a},m}(1)-F'_{\mathrm{a},m}(0)\right\}\tag{37}$$

or

$$\psi_{\mathrm{F,cd}} = \frac{-\int_0^1 v_{\mathrm{d}} W_{\mathrm{d}} B \psi_{\mathrm{d}}(\eta_{\mathrm{d}}, 0)\,\mathrm{d}\eta_{\mathrm{d}}}{V} = \frac{-W}{W_{\mathrm{d}} Gz} \sum_{m=0}^{\infty} \frac{\mathrm{e}^{-\lambda_m} S_{\mathrm{d},m}}{\lambda_m} \left\{ F'_{\mathrm{d},m}(1) - F'_{\mathrm{d},m}(0) \right\} \tag{38}$$

or may be examined by Eq. (41), which is readily obtained from the following overall energy balance on the outer tube:

$$V(1-\psi_{\mathrm{F,ab}}) + V(1-\psi_{\mathrm{F,cd}}) = \int_0^1 \frac{\alpha BL}{W_{\mathrm{a}}} \frac{\partial \psi_{\mathrm{a}}(0,\xi)}{\partial \eta_{\mathrm{a}}}\,\mathrm{d}\xi + \int_0^1 \frac{\alpha BL}{W_{\mathrm{d}}} \frac{\partial \psi_{\mathrm{d}}(0,\xi)}{\partial \eta_{\mathrm{d}}}\,\mathrm{d}\xi \tag{39}$$

thus,

$$(1-\psi_{\mathrm{F,ab}}) + (1-\psi_{\mathrm{F,cd}}) = \frac{1}{Gz}\left[ \sum_{m=0}^{\infty} S_{\mathrm{a},m} F'_{\mathrm{a},m}(0) \frac{(1-\mathrm{e}^{-\lambda_m})W}{\lambda_m W_{\mathrm{a}}} + \sum_{m=0}^{\infty} S_{\mathrm{d},m} F'_{\mathrm{d},m}(0) \frac{(1-\mathrm{e}^{-\lambda_m})W}{\lambda_m W_{\mathrm{d}}} \right] \tag{40}$$

or

$$\psi_{\mathrm{F,ab}} + \psi_{\mathrm{F,cd}} = 2 - \frac{1}{Gz}\left[ \sum_{m=0}^{\infty} S_{\mathrm{a},m} F'_{\mathrm{a},m}(0) \frac{(1-\mathrm{e}^{-\lambda_m})W}{\lambda_m W_{\mathrm{a}}} + \sum_{m=0}^{\infty} S_{\mathrm{d},m} F'_{\mathrm{d},m}(0) \frac{(1-\mathrm{e}^{-\lambda_m})W}{\lambda_m W_{\mathrm{d}}} \right]. \tag{41}$$

After the coefficients, $S_{\mathrm{a},m}$, $S_{\mathrm{b},m}$, $S_{\mathrm{c},m}$ and $S_{\mathrm{d},m}$ are obtained, the mixed inlet temperatures for flow pattern A are calculated by

$$\begin{aligned}
\psi_i(\eta_i, 0) &= \frac{(R/R+1)\left[\int_0^1 v_{\mathrm{b}i} W_{\mathrm{b}i} B \psi_i(\eta_i, 1)\,\mathrm{d}\eta_i\right] + V}{V(R+1)} \\
&= \frac{1}{R+1}\left[1 + \frac{W_i B}{V}\left(\frac{R}{R+1}\right) \sum_{m=0}^{\infty} S_{i,m} \int_0^1 v_i(\eta_i) F_{i,m}(\eta_i)\,\mathrm{d}\eta_i\right] \\
&\quad \times \frac{1}{R+1}\left[1 + \frac{W_i B}{V}\left(\frac{R}{R+1}\right)\left(\frac{L\alpha}{W_i^2}\right) \sum_{m=0}^{\infty} \frac{S_{i,m}}{\lambda_m}\left\{F'_{i,m}(1) - F'_{i,m}(0)\right\}\right] \\
&= \frac{1}{R+1}\left[1 + \frac{WB}{W_i Gz}\left(\frac{R}{R+1}\right) \sum_{m=0}^{\infty} \frac{S_{i,m}}{\lambda_m}\left\{F'_{i,m}(1) - F'_{i,m}(0)\right\}\right] \quad i = \mathrm{b}, \mathrm{c}.
\end{aligned} \tag{42}$$

Similarly, for flow pattern B, in Eq. (42) with $i = \mathrm{a}, \mathrm{d}$.

## 3. Temperature distributions in a single-pass device and a double-pass device

By following the same mathematical treatment performed in the previous works [15,16], except the types of a single-pass device and a double-pass device, as shown in Figs. 2(a) and (b), the outlet temperature for double-pass devices ($\theta_{\mathrm{F}}$) as well as for single-pass devices ($\theta_{0,\mathrm{F}}$) were also obtained in terms of the Graetz number ($Gz$), eigenvalues ($\lambda_m$ and $\lambda_{0,m}$),

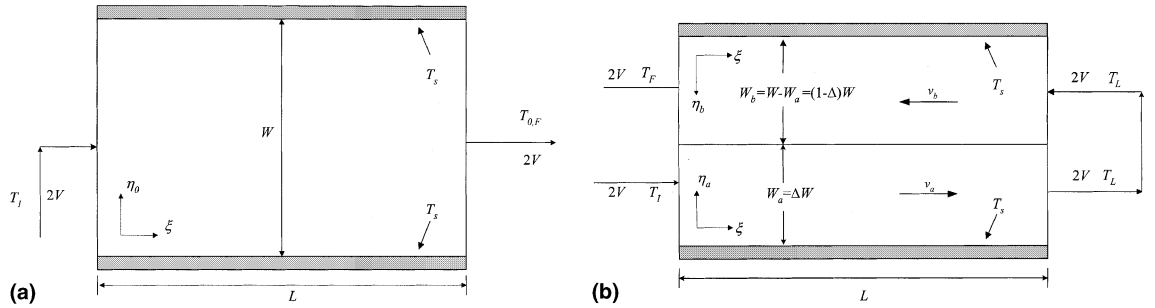


Fig. 2. (a) Single- and (b) double-pass heat exchangers.

expansion coefficients ($S_{a,m}$, $S_{b,m}$ and $S_{0,m}$), location of impermeable sheet ($\Delta$) and eigenfunctions ($F_{a,m}(\eta_a)$, $F_{b,m}(\eta_b)$ and $F_{0,m}(\eta_0)$). The results are

$$\theta_F = 1 - \psi_F = \frac{1}{Gz}\left[\sum_{m=0}^{\infty}\frac{(1-e^{-\lambda_m})}{\lambda_m \Delta}S_{a,m}F'_{a,m}(0) + \sum_{m=0}^{\infty}\frac{(1-e^{-\lambda_m})}{\lambda_m(1-\Delta)}S_{b,m}F'_{b,m}(0)\right], \tag{43}$$

$$\theta_{0,F} = 1 - \psi_{0,F} = \frac{1}{Gz}\sum_{m=0}^{\infty}\left[\frac{(1-e^{-\lambda_{0,m}})}{\lambda_{0,m}}S_{0,m}F'_{0,m}(0) - \frac{(1-e^{-\lambda_{0,m}})}{\lambda_{0,m}}S_{0,m}F'_{0,m}(1)\right]. \tag{44}$$

The results are represented in Figs. 5 and 6.

## 4. The improvement of transfer efficiency

The Nusselt number is defined as

$$\overline{Nu} = \frac{\overline{h}W}{k} \tag{45}$$

in which the average heat transfer coefficient is defined as

$$q = \overline{h}(2BL)(T_s - T_1). \tag{46}$$

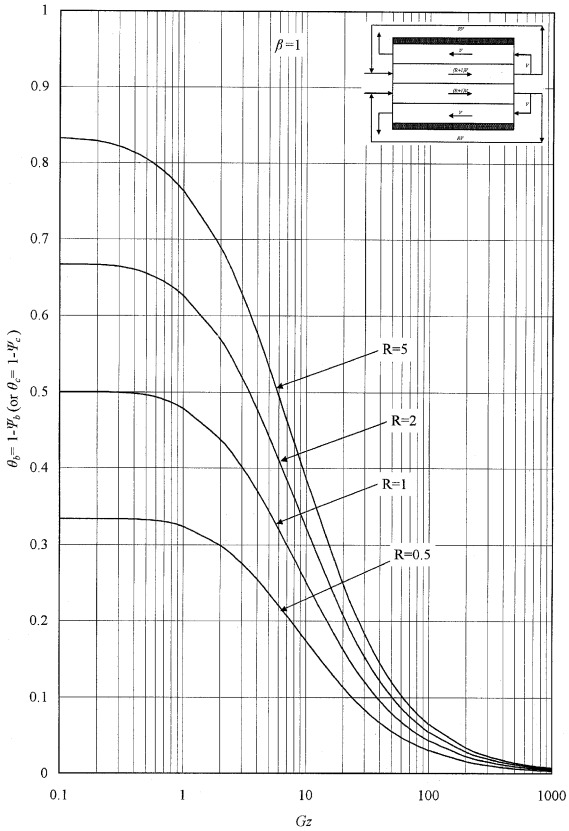


Fig. 3. Dimensionless average inlet temperatures of fluid after mixing. Reflux ratio as a parameter; $\beta = 1$ (flow pattern A).

Since

$$\overline{h}(2BL)(T_s - T_I) = V\rho c_p(T_F - T_I) \tag{47}$$

or

$$\overline{h} = \frac{V\rho c_p}{2BL}\left(\frac{T_F - T_I}{T_s - T_I}\right) = \frac{V\rho c_p}{2BL}(1 - \psi_F). \tag{48}$$

Thus

$$\overline{Nu} = \frac{\overline{h}W}{k} = \frac{VW}{2\alpha BL}(1 - \psi_F) = 0.5Gz(1 - \psi_F) = 0.5Gz\theta_F. \tag{49}$$

Similarly, for a single-pass device without recycle

$$\overline{Nu_0} = \frac{\overline{h_0}W}{k} = \frac{2VW}{2\alpha BL}(1 - \psi_{0,F}) = Gz(1 - \psi_{0,F}) = Gz\theta_{0,F}. \tag{50}$$

The improvement of heat transfer, $I_h$, for double- and four-pass devices by inserting the impermeable sheet with negligible thermal resistance are best illustrated by calculating the percentage increase in heat-transfer rate, based on the heat transfer of a single-pass operation of the same Graetz number without recycle as

$$I_h = \frac{\overline{Nu} - \overline{Nu_0}}{\overline{Nu_0}}\%. \tag{51}$$

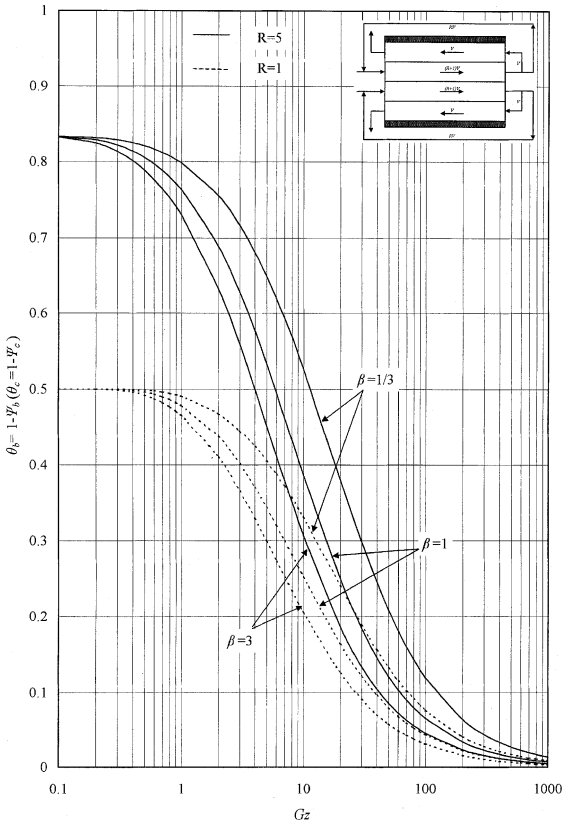


Fig. 4. Dimensionless average inlet temperatures of fluid after mixing. The ratio of channel thickness as a parameter; $R = 1$ and 5 (flow pattern A).

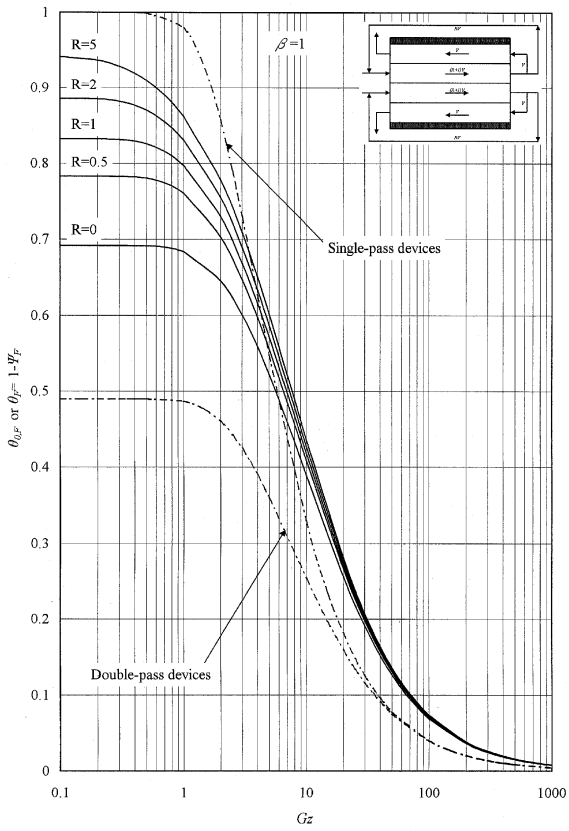


Fig. 5. Dimensionless outlet temperature vs. $Gz$ with reflux ratio as parameter; $\beta = 1$ (flow pattern A).

## 5. Increment of power consumption

### 5.1. Power consumption in the single-pass device

The friction loss in conduits may be estimated by

$$\ell w_{\mathrm{f}} = \frac{2f\,\overline{v}^2 L}{D_{\mathrm{e}}}, \tag{52}$$

where $\overline{v}$ and $D_{\mathrm{e}}$ denote the bulk velocity in the conduits and the equivalent diameters of the conduits, respectively, while $f = 16/Re$ is the friction factor which is the function of Reynolds number, $Re$. As an illustration, the power consumption of the single-pass device will be illustrated by the working dimensions as follows: $L = 1.2$ m, $W = 0.04$ m, $B = 0.2$ m, $V = 1 \times 10^{-5}$ m$^3$/s, $\mu = 8.94 \times 10^{-4}$ kg/m s, $\rho = 997.08$ kg/m$^3$. From these numerical values, the friction loss and hydraulic dissipated energy $P_0$ in conduit of a single-pass device was calculated by the appropriate equations and the results are

$$P_0 = 2V\rho(\ell w_{\mathrm{f},0}) = 1.073 \times 10^{-4}\ \mathrm{W} = 1.44 \times 10^{-7}\ \mathrm{hp}. \tag{53}$$

### 5.2. Increment of power consumption in double- and multi-pass devices

For double- and multi-pass devices, the average velocity of the fluid and equivalent diameter of conduit for flow pattern A are

$$\overline{v_0} = \frac{2V}{BW}, \quad \overline{v_{\mathrm{a}}} = \frac{V}{BW_{\mathrm{a}}}, \quad \overline{v_{\mathrm{b}}} = \frac{V(R+1)}{BW_{\mathrm{b}}}, \quad \overline{v_{\mathrm{c}}} = \frac{V(R+1)}{BW_{\mathrm{c}}}, \quad \overline{v_{\mathrm{d}}} = \frac{V}{BW_{\mathrm{d}}}, \tag{54}$$

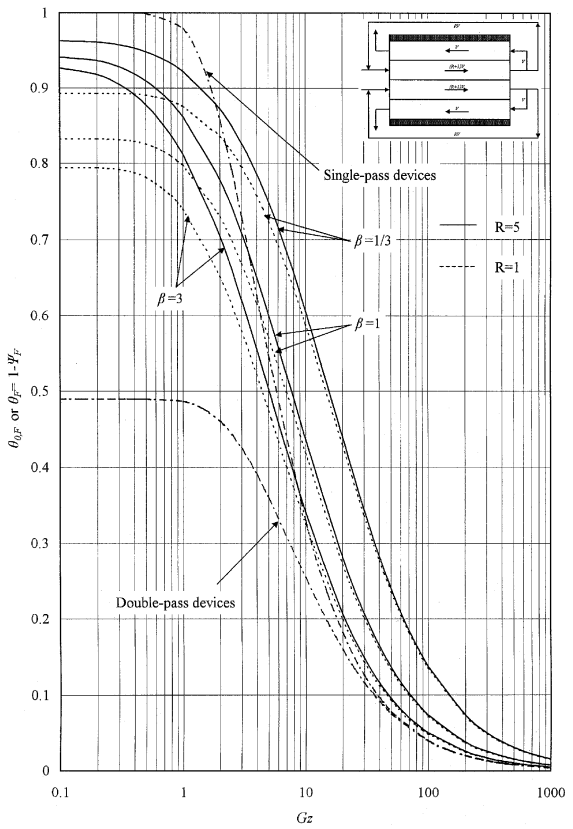


Fig. 6. Dimensionless outlet temperature vs. $Gz$ with $\beta$ as parameter; $R = 1$ and 5 (flow pattern A).

$$D_{e,0} = 2W, \quad D_{e,a} = 2W_a, \quad D_{e,b} = 2W_b, \quad D_{e,c} = 2W_c, \quad D_{e,d} = 2W_d. \tag{55}$$

Thus, from Eqs. (54) and (55), one obtains

$$R_{e0} = 2R_{e,a} = \frac{2}{(R+1)}R_{e,b} = \frac{2}{(R+1)}R_{e,c} = 2R_{e,d} \tag{56}$$

and then we have, for laminar flow

$$f_0 = \frac{1}{2}f_a = \frac{(R+1)}{2}f_b = \frac{(R+1)}{2}f_c = \frac{1}{2}f_d. \tag{57}$$

The increment of power consumption, $I_p$, may be defined as

$$I_p = \frac{P - P_0}{P_0} = \frac{[\ell w_{f,a} + (R+1)\ell w_{f,b} + (R+1)\ell w_{f,c} + \ell w_{f,d}] - (2\ell w_{f,0})}{2\ell w_{f,0}}, \tag{58}$$

where $P = V\rho[\ell w_{f,a} + (R+1)\ell w_{f,b} + (R+1)\ell w_{f,c} + \ell w_{f,d}]$.

Substitution of Eqs. (51)–(55) into Eq. (56) results in Eqs. (58) and (59) for flow pattern A and flow pattern B, respectively.

$$I_p = \frac{1}{2}\left(\frac{W}{W_a}\right)^3 + \frac{1}{2}(R+1)^2\left(\frac{W}{W_b}\right)^3 - 1, \tag{59}$$

$$I_p = \frac{1}{2}(R+1)^2\left(\frac{W}{W_a}\right)^3 + \frac{1}{2}\left(\frac{W}{W_b}\right)^3 - 1. \tag{60}$$

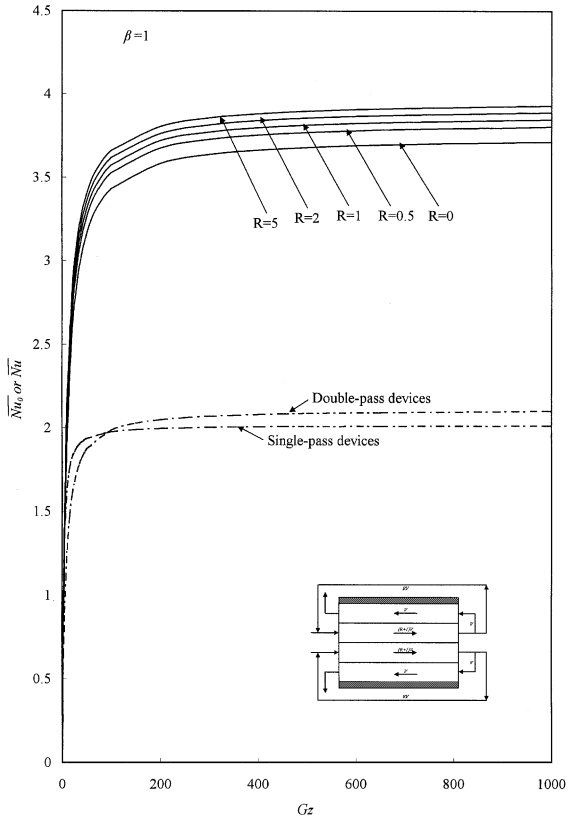


Fig. 7. Average Nusselt number vs. $Gz$ with reflux ratio as parameter; $\beta = 1$ (flow pattern A).

Similarly, for a double-pass device

$$I_p = \frac{1}{\Delta^3} + \frac{1}{(1-\Delta)^3} - 1. \tag{61}$$

It is readily obtained from Eq. (61) that $I_p = 1000$, 36 and 15 for $\Delta = 0.1$ (or 0.9), 0.3 (or 0.7) and 0.5, respectively. Some results for $I_p$ of multi-pass device are presented in Tables 4 and 5 for flow pattern A and flow pattern B, respectively. It is seen from this table that the increment of power consumption does not depend on Graetz number but increases with the reflux ratio or as $\beta$ goes away from 1, especially for $\beta > 1$ in flow pattern A and $\beta < 1$ in flow pattern B.

## 6. Results and discussion

The equation of multi-pass heat exchangers with external refluxes has been developed and solved by the use of the orthogonal expansion technique. Table 1 shows some calculation results of the first two eigenvalues and their associated expansion coefficients, as well as the dimensionless outlet temperatures, for $\beta = 1$, $R = 1$, and $Gz = 1$, 10, 100 and 1000. It was observed that due to the rapid convergence, only the first negative eigenvalues is necessary to be considered during the calculation of temperature distributions.

### 6.1. Flow pattern A

The mixed dimensionless inlet temperature increases with the amount of the reflux fluid (or reflux ratio), and the temperature of reflux fluid increases with the residence time which is inversely proportional to the inlet volume rate (or the Graetz number). Accordingly, it is shown in Figs. 3 and 4 that the dimensionless inlet temperature of fluid after

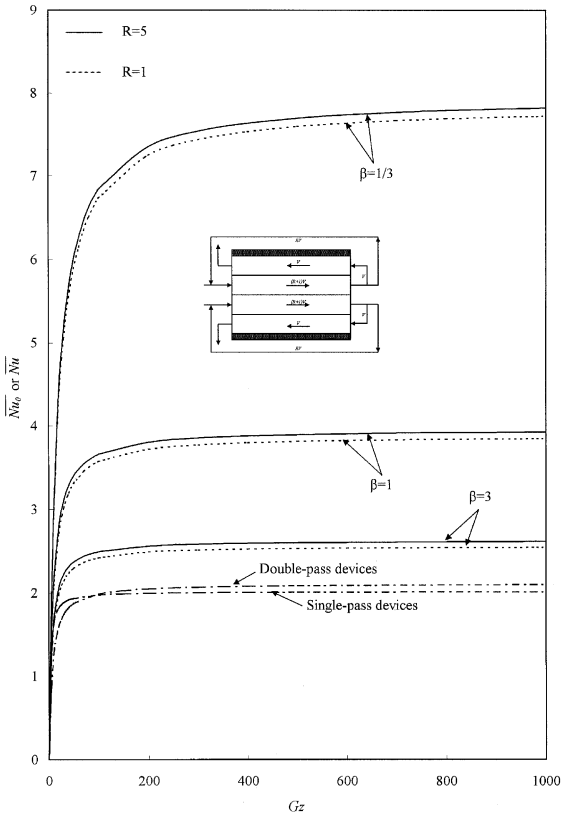


Fig. 8. Average Nusselt number vs. $Gz$ with $\beta$ as parameter; $R = 1$ and 5 (flow pattern A).

mixing increases with reflux ratio and with decreasing $\beta$ but decreases with Graetz number. Although the recycle-effect has positive influences on heat transfer, the preheating effect by increasing the reflux ratio cannot compensate for the decrease of residence time at low Graetz number, and hence the outlet temperature (or heat transfer) decreases with increasing reflux ratio. The comparison of dimensionless outlet temperatures, $\theta_F$ and $\theta_{0,F}$, as well as average Nusselt numbers, $\overline{Nu}$ and $\overline{Nu_0}$, may be observed from Figs. 5–8. Fig. 5 shows another more practical form of dimensionless outlet temperature $\theta_F$ (or $\theta_{0,F}$) vs. $Gz$ with the reflux ratio $R$ as a parameter for $\beta = 1$ while Fig. 6 with the ratio of channel thickness $\beta$ as a parameter. It was also found in Figs. 5 and 6 and Table 2 that the dimensionless average outlet temperature decreases with increasing the Graetz number $Gz$ owing to the short residence time of fluid, but increases as the reflux ratio $R$ increases, due to the preheating effect, or when the ratio of channel thickness $\beta$ decreases, due to the creation of high convective heat-transfer coefficient in channel a (and channel d) where the temperature difference between the heated plate and fluid is larger than in channel b (and channel c). It is seen from Figs. 5 and 6 that the difference $(\theta_F - \theta_{0,F})$ of outlet temperatures decreases with $Gz$, and then turns to decreasing with any values of $R$ and $\beta$. The Nusselt numbers ($\overline{Nu}$ and $\overline{Nu_0}$) and hence the improvement of transfer efficiencies ($I_h$) are proportional to $\theta_F$ (or $\theta_{0,F}$), as shown in Eqs. (55)–(57), so the higher improvement of performance is really obtained by employing a four-pass

Table 2
The improvement of the transfer efficiency with reflux ratio and sheetposition as parameters (flow pattern A)

| $I_h$ (%) | $R = 1$ | | | $R = 2$ | | | $R = 5$ | | |
|---|---|---|---|---|---|---|---|---|---|
| | $\beta = 1/3$ | $\beta = 1$ | $\beta = 3$ | $\beta = 1/3$ | $\beta = 1$ | $\beta = 3$ | $\beta = 1/3$ | $\beta = 1$ | $\beta = 3$ |
| $Gz = 1$ | −10.54 | −18.58 | −24.49 | −8.04 | −15.09 | −20.56 | −5.79 | −11.94 | −17.05 |
| $Gz = 10$ | 78.71 | 26.92 | −1.51 | 81.46 | 29.69 | 1.00 | 84.17 | 32.36 | 3.37 |
| $Gz = 100$ | 240.66 | 80.88 | 22.66 | 243.47 | 83.14 | 24.58 | 246.25 | 85.32 | 26.40 |
| $Gz = 1000$ | 283.48 | 90.98 | 26.58 | 285.99 | 93.06 | 28.38 | 288.46 | 95.07 | 30.09 |

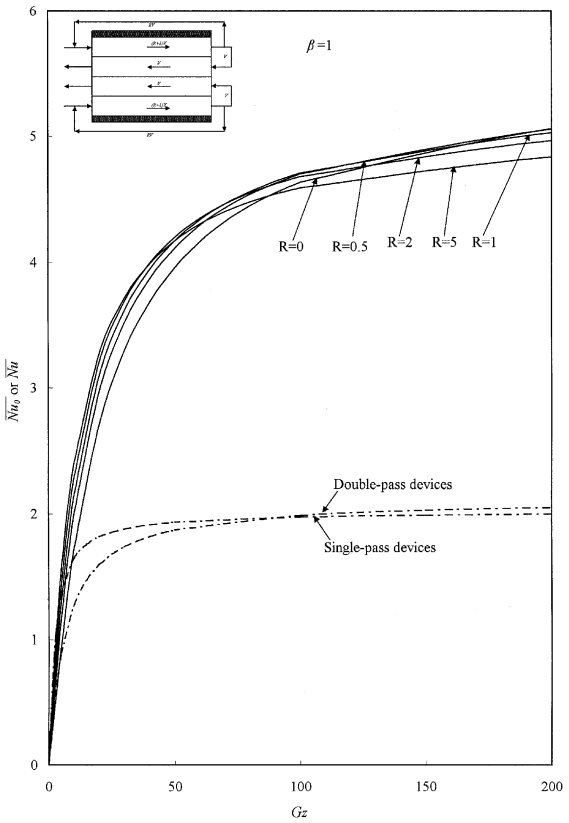


Fig. 9. Average Nusselt number vs. $Gz$ with reflux ratio as parameter; $\beta = 1$ (flow pattern B).

device, instead of using a single-pass device for large Graetz numbers and a double-pass device ($\beta = 0$ and $W_b = W_c = W/2$) for all Graetz numbers, if the volumetric flow rate in all devices is kept the same. Fig. 7 shows the theoretical average Nusselt numbers $\overline{Nu}$ vs. $Gz$, with the reflux ratio as a parameter for $\beta = 1$ while Fig. 8 with reflux ratio and the ratio of the channel thickness $\beta$ as parameters. On the other hand, as shown in Fig. 7, $(\overline{Nu} - \overline{Nu_0})$ increases with $Gz$ or with reflux ratio $R$, but the increase with $Gz$ is limitted as $Gz$ approaches infinitly. It is concluded that Nusselt number increases with increasing $R$, but with decreasing Graetz number as well as the ratio of channel thickness $\beta$. Some numerical values of the improvement in performance $I_h$ were given in Table 2. The minus signs in Table 2 indicate that when $Gz = 1$, no improvement in transfer efficiency can be achieved for any $R$ and $\beta$, and in this case, the single-pass device without recycle is preferred to be employed rather than using the four-pass one with recycle operating at such conditions.

### 6.2. Flow pattern B

The calculation methods are similar to those in the previous section of flow pattern A. Theoretical average Nusselt numbers and improvement of the transfer efficiency with Graetz number, reflux ratio and the ratio of the thickness $\beta$ as parameters, as presented in Figs. 9 and 10 and Table 3, were obtained for flow pattern B in Fig. 1(b). One may notice in Fig. 9 and Table 3 that the values of Nusselt number increase with $R$ but the increase with $R$ is in the reverse order for $Gz > 200$. A comparison of Figs. 7 and 8 with Figs. 9 and 10 indicates an enhancement of heat-transfer rate occurs for flow pattern B. Tables 4 and 5 show that the power consumption calculated for both flow patterns by assuming only the friction losses to the walls were significant. Operation under these conditions, the theoretical predictions show that the friction losses estimated by Eqs. (59)–(61), actually are still small even for such high value of $\beta$ ($P = 1.328 \times 10^{-3}$ hp). However, the increment of power consumption in flow pattern B is higher than that in flow pattern A, especially for $\beta < 1$, and in designing both flow pattern A and flow pattern B with a proper selection of reflux ratio and the ratio of channel thickness should be economically feasible in the device of multi-pass heat exchangers.

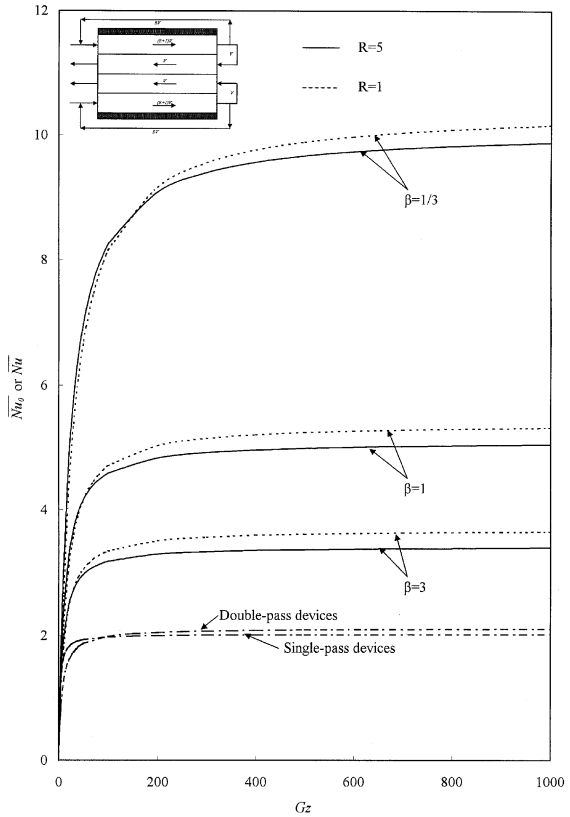


Fig. 10. Average Nusselt number vs. $Gz$ with $\beta$ as parameter; $R = 1$ and 5 (flow pattern B).

Table 3
The improvement of the transfer efficiency with reflux ratio and sheet position as parameters (flow pattern B)

| $I_h$ (%) | $R = 1$ | | | $R = 2$ | | | $R = 5$ | | |
|---|---|---|---|---|---|---|---|---|---|
| | $\beta = 1/3$ | $\beta = 1$ | $\beta = 3$ | $\beta = 1/3$ | $\beta = 1$ | $\beta = 3$ | $\beta = 1/3$ | $\beta = 1$ | $\beta = 3$ |
| $Gz = 1$ | −37.94 | −40.45 | −42.43 | −27.71 | −29.65 | −31.38 | −14.69 | −17.00 | −19.68 |
| $Gz = 10$ | 62.11 | 30.33 | 9.35 | 76.39 | 38.77 | 14.85 | 89.94 | 45.72 | 18.35 |
| $Gz = 100$ | 313.23 | 138.14 | 69.46 | 317.04 | 136.76 | 66.71 | 318.12 | 132.23 | 61.11 |
| $Gz = 1000$ | 404.00 | 164.11 | 81.45 | 398.62 | 159.01 | 76.51 | 390.22 | 150.62 | 68.72 |

Table 4
The increment of power consumption with reflux ratio and sheet position as parameters (flow pattern A)

| $I_p$ | | | |
|---|---|---|---|
| $R$ | $\beta = 1/3$ | $\beta = 1$ | $\beta = 3$ |
| 0.5 | 276.42 | 103 | 584.52 |
| 1 | 293.07 | 159 | 1032.52 |
| 2 | 340.65 | 319 | 2312.52 |
| 5 | 597.61 | 1183 | 9224.52 |

Table 5
The increment of power consumption with reflux ratio and sheet position as parameters (flow pattern B)

| $I_p$ | | | |
|---|---|---|---|
| $R$ | $\beta = 1/3$ | $\beta = 1$ | $\beta = 3$ |
| 0.5 | 584.52 | 103 | 276.42 |
| 1 | 1032.52 | 159 | 293.07 |
| 2 | 2312.52 | 319 | 340.65 |
| 5 | 9224.52 | 1183 | 597.61 |

## 7. Conclusion

Heat transfer through multi-pass parallel-plate operations with an impermeable sheet of negligible thermal resistance have been investigated and solved analytically by the use of the orthogonal expansion technique with the eigenfunction expanding in terms of an extended power series. The methods for improving the performance in heat transfer device are either in the double-pass operation by inserting an impermeable sheet or in the multi-pass operation by inserting three impermeable sheets with negligible thermal resistance. Application of the recycle-effect concept in designing a multi-pass heat exchanger is technically and economically feasible. Moreover, further improvement in transfer efficiency may be obtained if the smaller ratio of channel thickness $\beta$ is selected. The comparison of transfer efficiencies between multi-pass devices and a single-pass device is readily observed from Figs. 7 and 9 and Tables 2 and 3. The improvement of performance is really obtained by employing multi-pass devices, instead of using a single-pass device of same size without recycle, and the improvement increases with increasing the Graetz number and reflux ratio, as well as with decreasing the ratio of channel thickness. The reason why the improvement increases with decreasing the ratio of channel thickness may be considered as that the enhancement of heat transfer in outer channel due to decreasing the thickness of the outer channel to increase the flow velocity can compensate for the decrease of heat transfer in the inner channel with reflux ratio $R$ due to driving force in outer channel is larger than that in inner channel, leading to improved performance.

There are several possible arrangements with different types of refluxes, each type of reflux results in improving heat transfer efficiencies with Graetz number of interest, a suitable selection of the type of reflux would be come out an evident advantage for practical applications. It is apparent that the mathematical treatments developed in this study are only conducted in a heat-transfer sense with constant wall temperature, the present theory and method may also be applied to other conjugated Graetz problems in heat-or mass-transfer devices with constant heat flux or mass flux on the boundary.

## Acknowledgements

The author wishes to thank the National Science Council of the Republic of China for the financial support.

## Appendix A

Eq. (14) can be rewritten as

$$F''_{a,m}(\eta_a) - G_{z,m}(R+1)\frac{W_a}{W}(6\eta_a - 6\eta_a^2)F_{a,m}(\eta_a) = 0, \tag{A.1}$$

$$F''_{b,m}(\eta_b) + G_{z,m}\frac{W_b}{W}(6\eta_b - 6\eta_b^2)F_{b,m}(\eta_b) = 0, \tag{A.2}$$

$$F''_{d,m}(\eta_d) - G_{z,m}(R+1)\frac{W_d}{W}(6\eta_d - 6\eta_d^2)F_{d,m}(\eta_d) = 0, \tag{A.3}$$

$$F''_{c,m}(\eta_c) + G_{z,m}\frac{W_c}{W}(6\eta_c - 6\eta_c^2)F_{c,m}(\eta_c) = 0. \tag{A.4}$$

Combining Eqs. (A.1)–(A.4) and (15)–(26) yields

$$p_{m,2}=0,\quad p_{m,3}=0,\quad p_{m,4}=\frac{1}{2}\lambda_m G_z(R+1)\frac{W_a}{W},\ldots,\quad p_{m,n}=\frac{6\lambda_m G_z(R+1)(p_{m,n-3}-p_{m,n-4})}{n(n-1)}\frac{W_a}{W}, \tag{A.5}$$

$$q_{m,2}=0,\quad q_{m,3}=-\lambda_m G_z\frac{W_b}{W}q_{m,0},\ldots,\quad q_{m,n}=-\frac{6\lambda_m G_z(q_{m,n-3}-q_{m,n-4})}{n(n-1)}\frac{W_b}{W}, \tag{A.6}$$

$$r_{m,2}=0,\quad r_{m,3}=-\lambda_m G_z\frac{W_c}{W}r_{m,0},\ldots,\quad r_{m,n}=-\frac{6\lambda_m G_z(r_{m,n-3}-r_{m,n-4})}{n(n-1)}\frac{W_c}{W}, \tag{A.7}$$

$$t_{m,2}=0,\quad t_{m,3}=0,\quad t_{m,4}=\frac{1}{2}\lambda_m G_z(R+1)\frac{W_d}{W},\ldots,\quad t_{m,n}=\frac{6\lambda_m G_z(R+1)(t_{m,n-3}-t_{m,n-4})}{n(n-1)}\frac{W_d}{W}. \tag{A.8}$$

## Appendix B

A demonstration of completeness and its justification based on Sturm–Liouville theorem
From Eq. (14) with $i=\mathrm{a}$

$$S_{a,m}F''_{a,m}(\eta_a)-\lambda_m\left[\frac{W_a^2 v_a(\eta_a)}{L\alpha}\right]S_{a,m}F_{a,m}(\eta_a)=0, \tag{B.1}$$

$$S_{a,n}F''_{a,n}(\eta_a)-\lambda_n\left[\frac{W_a^2 v_a(\eta_a)}{L\alpha}\right]S_{a,n}F_{a,n}(\eta_a)=0. \tag{B.2}$$

Multiplying Eq. (B.1) by $S_{a,n}F_{a,n}$ and Eq. (B.2) by $S_{a,m}F_{a,m}$, and subtract the results get

$$S_{a,m}S_{a,n}\left[F_{a,n}(\eta_a)F''_{a,m}(\eta_a)-F_{a,m}(\eta_a)F''_{a,n}(\eta_a)\right]+(\lambda_n-\lambda_m)\left[\frac{W_a^2 v_a(\eta_a)}{L\alpha}\right]S_{a,m}S_{a,n}F_{a,n}F_{a,m}=0. \tag{B.3}$$

Integrating over the region of interest gives

$$\int_0^1 S_{a,m}S_{a,n}\left[F_{a,n}F''_{a,m}-F_{a,m}F''_{a,n}\right]\mathrm{d}\eta_a+(\lambda_n-\lambda_m)\int_0^1\left[\frac{W_a^2 v_a(\eta_a)}{L\alpha}\right]S_{a,m}S_{a,n}F_{a,n}F_{a,m}\,\mathrm{d}\eta_a=0. \tag{B.4}$$

Integrating by parts in the first term of Eq. (B.4) gives

$$\begin{aligned}\int_0^1 S_{a,m}S_{a,n}\left[F_{a,n}F''_{a,m}-F_{a,m}F''_{a,n}\right]\mathrm{d}\eta_a&=S_{a,m}S_{a,n}\left[F_{a,n}F'_{a,m}-F_{a,m}F'_{a,n}\right]_0^1-\int_0^1 S_{a,m}S_{a,n}\left[F'_{a,n}F'_{a,m}-F'_{a,m}F'_{a,n}\right]\mathrm{d}\eta_a\\&=S_{a,m}S_{a,n}\left[F_{a,n}F'_{a,m}-F_{a,m}F'_{a,n}\right]_0^1.\end{aligned} \tag{B.5}$$

Then Eq. (B.4) can be rewritten as

$$S_{a,m}S_{a,n}\left[F_{a,n}F'_{a,m}-F_{a,m}F'_{a,n}\right]_0^1+(\lambda_n-\lambda_m)\int_0^1\left[\frac{W_a^2 v_a(\eta_a)}{L\alpha}\right]S_{a,m}S_{a,n}F_{a,n}F_{a,m}\,\mathrm{d}\eta_a=0 \tag{B.6}$$

Similarly, one can obtain the same equations for subchannels b, c and d as follows:

$$S_{b,m}S_{b,n}\left[F_{b,n}F'_{b,m}-F_{b,m}F'_{b,n}\right]_0^1+(\lambda_n-\lambda_m)\int_0^1\left[\frac{W_b^2 v_b(\eta_b)}{L\alpha}\right]S_{b,m}S_{b,n}F_{b,n}F_{b,m}\,\mathrm{d}\eta_b=0, \tag{B.7}$$

$$S_{c,m}S_{c,n}\left[F_{c,n}F'_{c,m}-F_{c,m}F'_{c,n}\right]_0^1+(\lambda_n-\lambda_m)\int_0^1\left[\frac{W_c^2 v_c(\eta_c)}{L\alpha}\right]S_{c,m}S_{c,n}F_{c,n}F_{c,m}\,\mathrm{d}\eta_c=0, \tag{B.8}$$

$$S_{d,m}S_{d,n}\left[F_{d,n}F'_{d,m}-F_{d,m}F'_{d,n}\right]_0^1+(\lambda_n-\lambda_m)\int_0^1\left[\frac{W_d^2 v_d(\eta_d)}{L\alpha}\right]S_{d,m}S_{d,n}F_{d,n}F_{d,m}\,\mathrm{d}\eta_d=0. \tag{B.9}$$

Multiplying Eq. (B.6) by $W_b W_c W_d$, Eq. (B.7) by $W_c W_d W_a$, Eq. (B.8) by $W_d W_a W_b$ and Eq. (B.9) by $W_a W_b W_c$, and add the results yield

$$W_b W_c W_d S_{a,m} S_{a,n} [F_{a,n} F'_{a,m} - F_{a,m} F'_{a,n}]_0^1 + W_b W_c W_d (\lambda_n - \lambda_m) \int_0^1 \left[ \frac{W_a^2 v_a(\eta_a)}{L\alpha} \right] S_{a,m} S_{a,n} F_{a,n} F_{a,m} \, d\eta_a$$
$$+ W_c W_d W_a S_{b,m} S_{b,n} [F_{b,n} F'_{b,m} - F_{b,m} F'_{b,n}]_0^1 + W_c W_d W_a (\lambda_n - \lambda_m) \int_0^1 \left[ \frac{W_b^2 v_b(\eta_b)}{L\alpha} \right] S_{b,m} S_{b,n} F_{b,n} F_{b,m} \, d\eta_b$$
$$+ W_d W_a W_b S_{c,m} S_{c,n} \left[ F_{c,n} F'_{c,m} - F_{c,m} F'_{c,n} \right]_0^1 + W_d W_a W_b (\lambda_n - \lambda_m) \int_0^1 \left[ \frac{W_c^2 v_c(\eta_c)}{L\alpha} \right] S_{c,m} S_{c,n} F_{c,n} F_{c,m} \, d\eta_c$$
$$+ W_a W_b W_c S_{d,m} S_{d,n} \left[ F_{d,n} F'_{d,m} - F_{d,m} F'_{d,n} \right]_0^1 + W_a W_b W_c (\lambda_n - \lambda_m) \int_0^1 \left[ \frac{W_d^2 v_d(\eta_d)}{L\alpha} \right] S_{d,m} S_{d,n} F_{d,n} F_{d,m} \, d\eta_d = 0 \quad \text{(B.10)}$$

using Eqs. (15)–(22) in Eq. (B.10) and with $\lambda_n \neq \lambda_m$ give the orthogonality conditions as shown in Eq. (30).

## References


[1] R.K. Shah, A.L. London, in: Laminar Flow Forced Convection in Ducts, Academic Press, New York, 1978, pp. 196–207.
[2] V.-D. Dang, M. Steinberg, Convective diffusion with homogeneous and heterogeneous reaction in a tube, J. Phys. Chem. 84 (1980) 214–219.
[3] J.R. Sellars, M. Tribus, J.S. Klein, Heat transfer to laminar flow in a round tube or flat conduit – the Graetz problem extended, Trans. Am. Soc. Mech. Eng. 78 (1956) 441–448.
[4] A.P. Hatton, A. Quarmby, Heat transfer in the thermal entry length with laminar flow in an annulus, Int. J. Heat Mass Transfer 5 (1962) 973–980.
[5] M.L. Michelsen, J. Villadsen, The Graetz problem with axial heat conduction, Int. J. Heat Mass Transfer 17 (1974) 1391–1402.
[6] E. Papoutsakis, D. Ramkrishna, H.C. Lim, The extended Graetz problem with prescribed wall flux, AIChE J. 26 (1980) 779–787.
[7] T.L. Perelman, On conjugated problems of heat transfer, Int. J. Heat Mass Transfer 3 (1961) 293–303.
[8] D. Murkerjee, E.J. Davis, Direct-contact heat transfer immiscible fluid layers in laminar flow, AIChE J. 18 (1972) 94–101.
[9] S.S. Kim, D.O. Cooney, Improved theory for hollow-fiber enzyme reactor, Chem. Eng. Sci. 31 (1976) 289–294.
[10] E.J. Davis, S. Venkatesh, The solution of conjugated multiphase heat and mass transfer problems, Chem. Eng. Sci. 34 (1979) 775–787.
[11] E. Papoutsakis, D. Ramkrishna, Conjugated Graetz problems. I: general formalism and a class of solid–fluid problems, Chem. Eng. Sci. 36 (1981) 1381–1390.
[12] E. Papoutsakis, D. Ramkrishna, Conjugated Graetz problems. II: fluid–fluid problems, Chem. Eng. Sci. 36 (1981) 1393–1399.
[13] X. Yin, H.H. Bau, The conjugated Graetz problem with axial conduction, Trans. ASME 118 (1996) 482–485.
[14] H.M. Yeh, S.W. Tsai, C.L. Chiang, Recycle effects on heat and mass transfer through a parallel-plate channel, AIChE J. 33 (1987) 1743–1746.
[15] C.D. Ho, H.M. Yeh, W.S. Sheu, An analytical study of heat and mass transfer through a parallel-plate channel with recycle, Int. J. Heat Mass Transfer 41 (1998) 2589–2599.
[16] C.D. Ho, H.M. Yeh, W.S. Sheu, The influence of recycle on double-pass heat and mass transfer through a parallel-plate device, Int. J. Heat Mass Transfer 42 (1999) 1707–1722.
[17] S.N. Singh, The determination of eigen-functions of a certain Sturm–Liouville equation and its application to problems of heat-transfer, Appl. Sci. Res. (Section A) 32 (1958) 237–250.
[18] G.M. Brown, Heat or mass transfer in a fluid in laminar flow in a circular or flat conduit, AIChE J. 6 (1960) 179–183.
[19] R.J. Nunge, W.N. Gill, An analytical study of laminar counterflow double-pipe heat exchangers, AIChE J. 12 (1966) 279–289.
[20] R.J. Nunge, E.W. Porta, W.N. Gill, Axial conduction in the fluid streams of multistream heat exchangers, Chem. Eng. Progr. Symp. Series 63 (1967) 80–91.
[21] S.W. Tsai, H.M. Yeh, A study of the separation efficiency in horizontal thermal diffusion columns with external refluxes, Can. J. Chem. Eng. 63 (1985) 406–411.
[22] H.M. Yeh, S.W. Tsai, C.S. Lin, A study of the separation efficiency in thermal diffusion columns with a vertical permeable barrier, AIChE J. 32 (1986) 971–980.
[23] H.M. Yeh, S.W. Tsai, T.W. Chang, A study of the Graetz problem in concentric-tube continuous-contact countercurrent separation processes with recycles at both ends, Sep. Sci. Technol. 21 (1986) 403–419.
[24] M.A. Ebadian, H.Y. Zhang, An exact solution of extended Graetz problem with axial heat conduction, Int. J. Heat Mass Transfer 32 (1989) 1709–1717.
[25] J. Korpijarvi, P. Oinas, J. Reunanen, Hydrodynamics and mass transfer in airlift reactor, Chem. Eng. Sci. 54 (1998) 2255–2262.
[26] E. Santacesaria, M. Di Serio, P. Iengo, Mass transfer and kinetics in ethoxylation spray tower loop reactors, Chem. Eng. Sci. 54 (1999) 1499–1504.

[27] E. Garcia-Calvo, A. Rodriguez, A. Prados, J. Klein, Fluid dynamic model for three-phase airlift reactors, Chem. Eng. Sci. 54 (1998) 2359–2370.
[28] M. Atenas, M. Clark, V. Lazarova, Holdup and liquid circulation velocity in a rectangular air-lift bioreactor, Indus. Eng. Chem. Res. 38 (1999) 944–949.
[29] S. Goto, P.D. Gaspillo, Effect of static mixer on mass transfer in draft tube bubble column and in external loop column, Chem. Eng. Sci. 47 (1992) 3533–3539.
[30] K.I. Kikuchi, H. Takahashi, Y. Takeda, F. Sugawara, Hydrodynamic behavior of single particles in a draft-tube bubble column, Can. J. Chem. Eng. 77 (1999) 573–578.